

PCCP

Accepted Manuscript



This is an *Accepted Manuscript*, which has been through the Royal Society of Chemistry peer review process and has been accepted for publication.

Accepted Manuscripts are published online shortly after acceptance, before technical editing, formatting and proof reading. Using this free service, authors can make their results available to the community, in citable form, before we publish the edited article. We will replace this *Accepted Manuscript* with the edited and formatted *Advance Article* as soon as it is available.

You can find more information about *Accepted Manuscripts* in the [Information for Authors](#).

Please note that technical editing may introduce minor changes to the text and/or graphics, which may alter content. The journal's standard [Terms & Conditions](#) and the [Ethical guidelines](#) still apply. In no event shall the Royal Society of Chemistry be held responsible for any errors or omissions in this *Accepted Manuscript* or any consequences arising from the use of any information it contains.

Mechanistic Aspects of the Gas-Phase Coupling of Thioanisole and Chlorobenzene to Dibenzothiophene Catalyzed by Atomic Ho^+

Cite this: DOI: 10.1039/x0xx00000x

Received 00th January 2015,
Accepted 00th January 2015

DOI: 10.1039/x0xx00000x

www.rsc.org/

Shaodong Zhou, Maria Schlangen, and Helmut Schwarz*

Dedicated to Professor R. N. Zare, Stanford University, on the occasion of his 75th birthday.

Mechanistic aspects of the novel gas-phase generation of dibenzothiophene via coupling of thioanisole and chlorobenzene, employing atomic Ho^+ as a catalyst, have been investigated using Fourier-transform ion cyclotron resonance mass spectrometry in conjunction with density functional theory (DFT) calculations.

Introduction

Sulfur heterocycles are important building blocks of various chemical products, including organic thin-film transistors^{1,2}, metal extracting reagents^{3,4}, or bioactive and medicinally relevant compounds⁵⁻⁸. Consequently, methodological aspects related to the formation of organosulfur heterocyclic rings have attracted much attention. For the synthesis of sulfur-containing heterocycles usually metal sulfides, thioesters, or thioethers are employed as starting materials, and first- or second- row transition-metal complexes serve as catalysts. To achieve C–C⁹⁻¹² or C–S¹³⁻²⁰ coupling involved in the ring closure process, activation of C–H⁹⁻²⁰, C–X (X = Br or I)^{15,18,20} or C–S^{14,17} bonds is a prerequisite. While gas-phase investigations proved helpful to obtain mechanistic aspects for numerous processes, except for a few reports on the formation of sulfur heterocycles in the gas phase²¹, a more detailed understanding of the elementary steps is lacking.

In a previous study on the reactions of atomic Ln^+ with chlorobenzene²², strong indications have been found that Ho^+ generates efficiently the insertion product $\text{Ho}(\text{C}_6\text{H}_5)(\text{Cl})^+$ which then

promotes HCl elimination in a secondary reaction with chlorobenzene; further, intriguing coupling processes have been observed in preliminary studies on consecutive reactions of Ln^+ with chlorobenzene and thioanisole in which Ho^+ exhibited the highest efficiency. Thus, we explored these reactions in more detail, and here we describe a gas-phase approach of sequential C–C and C–S coupling to generate dibenzothiophene by using thioanisole and chlorobenzene as substrates and exploiting atomic Ho^+ as a catalyst. Gas-phase studies employing atomic catalysts²³ recently regained interest²⁴ in the context of “single-atom catalysis”²⁵.

Results and Discussion

Coupling of thioanisole and chlorobenzene is achieved via two steps: First, Ho^+ reacts with thioanisole to produce an ionic precursor, which subsequently undergoes reaction with chlorobenzene to re-generate Ho^+ under the elimination of the neutral heterocyclic product.

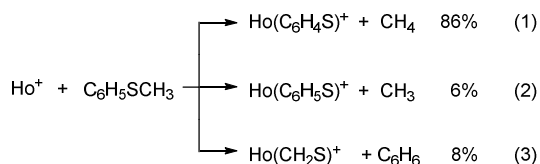
1 Reactions of Ho^+ with Thioanisole

1.1 Ion/molecule Reactions of Ho^+ with Thioanisole

Institut für Chemie, Technische Universität Berlin, Straße des 17. Juni 135, 10623 Berlin, Germany. Email: helmut.schwarz@tu-berlin.de.

†Electronic Supplementary Information (ESI) available: Experimental & computational details, and Figures. See DOI: 10.1039/b000000x/

Three primary channels were observed in the thermal reaction of Ho^+ with thioanisole introduced via a leak valve at a stationary pressure of $p = 1.0 \times 10^{-8}$ bar, i.e. reactions (1) – (3); the overall efficiency amounts to 30%, relative to the collision rate²⁶.



C–S bond activation is involved in all three channels; in addition, C–H bond activation takes place in reactions (1) and (3), respectively. Structural information on the cationic product ions as well as mechanistic aspects of these processes were obtained from DFT calculations. The potential-energy surfaces (PESs) together with structural data of the associated intermediates and transition structures are shown in Fig. 1 for the generations of $\text{Ho}(\text{C}_6\text{H}_4\text{S})^+$ and $\text{Ho}(\text{C}_6\text{H}_5\text{S})^+$, and in Fig. 2 two alternative pathways for the formation of $\text{Ho}(\text{CH}_2\text{S})^+$ are presented.

1.2 Pathways to form $\text{Ho}(\text{C}_6\text{H}_4\text{S})^+$ and $\text{Ho}(\text{C}_6\text{H}_5\text{S})^+$

Several coordination modes, e.g. η^2 or η^6 coordination to the ring, attachment of the cation to the sulfur atom etc., have been taken into account for the generation of an encounter complex of Ho^+ with thioanisole; however, irrespective of all starting structures considered, as a result of the optimization, only **1** has been identified as encounter complex. In **1**, Ho^+ is η^2 coordinated to the sulfur and the *ipso*-carbon atom of the phenyl ring. This intermediate serves as the starting point for all three reaction channels (1) – (3). Subsequent to the adduct formation, the generations of both $\text{Ho}(\text{C}_6\text{H}_4\text{S})^+$ and $\text{Ho}(\text{C}_6\text{H}_5\text{S})^+$, reactions (1) and (2), proceed by the oxidative insertion of Ho^+ into the S–CH₃ bond thus forming intermediate **2**. Since ground state Ho^+ possesses a $4f^{11}5d^06s^1$ electronic configuration, one $4f$ electron of Ho^+ has to be promoted to a non- f valence orbital to allow the formation of **2** in which holmium is engaged in forming two σ bonds. NBO analysis of the IRC coordinates of **TS1/2** indicates that the electron promotion of Ho^+ from a $4f$ orbital to a non- f valence orbital occurs after cleavage of the S–CH₃ bond. Thus,

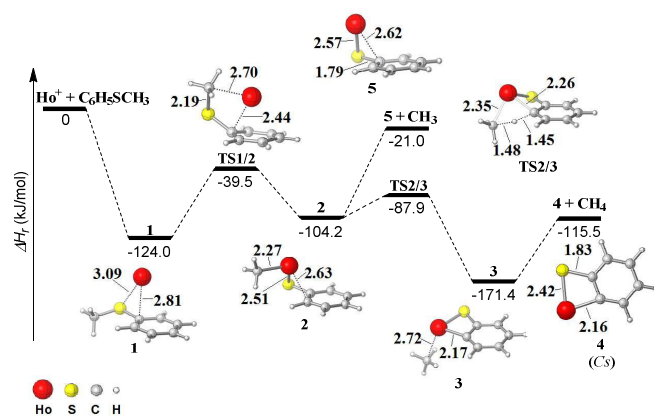


Fig. 1 PESs and structural information of the associated coordinates for the generations of $\text{Ho}(\text{C}_6\text{H}_4\text{S})^+$ and $\text{Ho}(\text{C}_6\text{H}_5\text{S})^+$. Selected bond lengths are given in Å; for the sake of clarity, charges are omitted.

both the promotion energy (PE) of Ho^+ to attain a $4f^{10}5d^16s^1$ configuration (158 kJ/mol^{27}) as well as the S–CH₃ bond dissociation energy ($BDE(\text{S–CH}_3)$, 278 kJ/mol^{28}) accompanied by distortion of the anisole molecule contribute to the energy barrier associated with **TS1/2**. While the homolytic cleavage of the Ho–CH₃ bond of intermediate **2** results in the formation of holmium benzenethiolate $\text{Ho}(\text{C}_6\text{H}_5\text{S})^+$ (**5**), generation of $\text{Ho}(\text{C}_6\text{H}_4\text{S})^+$ (**4**) proceeds via a metal mediated σ -bond metathesis process **2** → **3**, in which a hydrogen-atom transfer takes place from the *ortho*-position of the phenyl ring to the methyl group via **TS2/3**. Subsequently, the elimination of methane gives rise to the product ion **4**. In line with the experimental results, both reactions are exothermic and thus energetically accessible under thermal conditions; moreover, the preferred elimination of CH₄, observed in the experiments, agrees with the more energy demanding cleavage of the Ho–CH₃ bond of **2**, accompanied with the generation of $\text{Ho}(\text{C}_6\text{H}_5\text{S})^+$, as compared to the liberation of CH₄ along the sequence **2** → **3** → **4**. Considering the relative energies of **TS2/3** and **TS1/2** (-87.9 kJ/mol versus -39.5 kJ/mol), insertion of Ho^+ into the S–CH₃ bond constitutes the rate-limiting step for the generation of the major product $\text{Ho}(\text{C}_6\text{H}_4\text{S})^+$.

1.3 Generation of $\text{Ho}(\text{CH}_2\text{S})^+$

Two pathways have been located to produce $\text{Ho}(\text{CH}_2\text{S})^+$. The first one commences with insertion of Ho^+ into the S–C₆H₅ bond, while in the second one the CH₃S group remains bound in the migration of Ho^+ to the top of the phenyl ring. As mentioned above, for the insertion process one electron of Ho^+ has to be promoted from a $4f$ orbital to a non- f valence orbital; according to NBO analysis, the promotion takes place in proceeding from **TS1/7** to intermediate **7** after cleavage of the S–C₆H₅ bond; then, again, one electron re-occupies the $4f$ orbital of Ho^+ in the step **TS7/8** → **8**. In contrast, a $4f$ → non- f promotion is not necessary for the pathway initiated by migration of the whole CH₃SHo⁺ unit; here, throughout the reaction sequence **1** → **6** → **8** the holmium atom remains covalently bound only to the sulfur atom. Considering the comparable energies of **TS1/6**, **TS1/7**, and **TS6/8**, generation of $\text{Ho}(\text{CH}_2\text{S})^+$ is influenced by several factors, including the $BDE(\text{C}_6\text{H}_5\text{–S})$ (357 kJ/mol^{28}), and

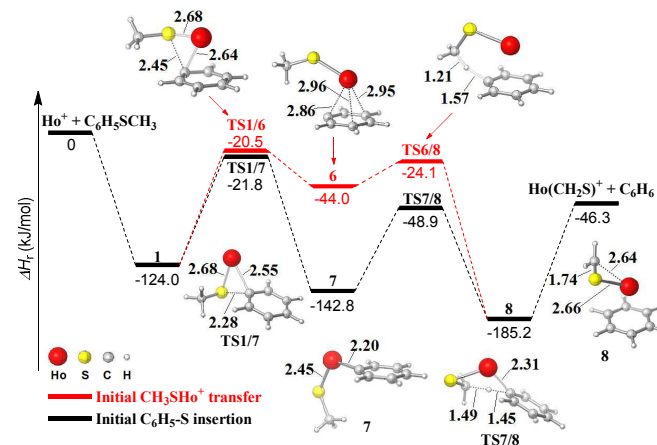
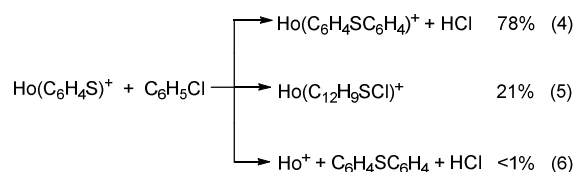


Fig. 2 PESs and structural information of the associated coordinates for the generation of $\text{Ho}(\text{CH}_2\text{S})^+$. Selected bond lengths are given in Å; for the sake of clarity, charges are omitted.

$BDE(\text{Ho}^+\text{SCH}_2\text{-H})$, as well as the PE of Ho^+ to attain a $4f^{10}5d^16s^1$ configuration. Finally, compared to the formation of $\text{Ho}(\text{C}_6\text{H}_4\text{S})^+$, the generation of $\text{Ho}(\text{CH}_2\text{S})^+$ is energetically less favorable, in agreement with its lower branching ratio; also, the energetics for the generations of $\text{Ho}(\text{C}_6\text{H}_5\text{S})^+$ and $\text{Ho}(\text{CH}_2\text{S})^+$ are in line with their similar branching ratios.

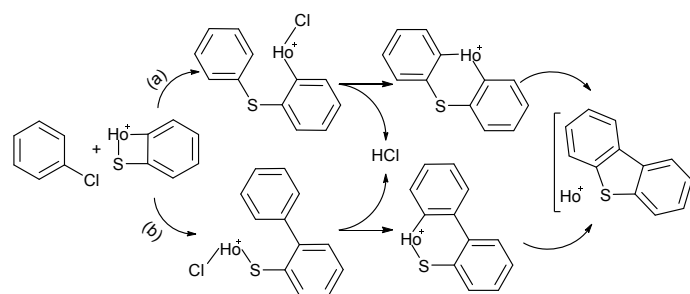
2 Reactions of $\text{Ho}(\text{C}_6\text{H}_4\text{S})^+$ with Chlorobenzene

For probing the thermal reactions of $\text{Ho}(\text{C}_6\text{H}_4\text{S})^+$ with chlorobenzene, the thermalized, mass-selected precursor $\text{Ho}(\text{C}_6\text{H}_4\text{S})^+$ is exposed to chlorobenzene which is introduced via a leak valve and present in the ICR cell at a stationary pressure of $p = 1.0 \times 10^{-8}$ bar. The overall reaction efficiency amounts to 7%, and three primary product channels were observed, i.e. reaction (4) – (6). Performing the same experiments without thermalization of the precursor $\text{Ho}(\text{C}_6\text{H}_4\text{S})^+$, the branching ratio of reaction (6) increases up to 27%, while the branching ratios of reaction (4) and (5) decrease to 63% and 10%, respectively.



The assignment of the $[\text{C}_{12}\text{H}_8\text{S}]$ unit as a dibenzothiophene ligand ($\text{C}_6\text{H}_4\text{SC}_6\text{H}_4$) in the product ion of reaction (4) as well as for the neutral molecule of reaction (6) is based on the following considerations. First, if $[\text{C}_{12}\text{H}_8\text{S}]$ corresponds to an intact $[\text{C}_{12}\text{H}_8\text{S}]$ ligand we assume a dibenzothiophene structure since the generation of isomeric naphthothiophene is much more complicated starting from the two substrates employed in the experiments. The next and even more important aspect concerns the question if $[\text{C}_{12}\text{H}_8\text{S}]$ represents a single ligand, or if it is composed of two individual units, e.g. $\text{C}_6\text{H}_4\text{S}$ and C_6H_4 . To this end, the major product ion $\text{Ho}(\text{C}_{12}\text{H}_8\text{S})^+$ has been mass selected and subjected to collision-induced dissociation (CID). At a collision energy $E_{\text{coll}} = 3.6$ eV (given in the center-of-mass frame), Ho^+ and HoS^+ are produced upon collision with argon in a ratio of about 9:1; applying lower collision energies, Ho^+ corresponds to the only fragment ion generated. From the above results, the following conclusions can be drawn: (i) $\text{Ho}(\text{C}_{12}\text{H}_8\text{S})^+$ corresponds to a complex with a single ligand which we assign to dibenzothiophene; the latter is generated in the reaction of thermalized $\text{Ho}(\text{C}_6\text{H}_4\text{S})^+$ with chlorobenzene under the elimination of HCl , and (ii) “bare” Ho^+ is formed as product ion via the consecutive eliminations of HCl and dibenzothiophene. Further, the alternative formation of $[\text{Ho}(\text{C}_6\text{H}_4\text{S})(\text{C}_6\text{H}_4)]^+$, possessing two individual ligands, e.g. $\text{C}_6\text{H}_4\text{S}$ and benzyne, would result in the formations of both fragment ions $\text{Ho}(\text{C}_6\text{H}_4\text{S})^+$ and $\text{Ho}(\text{C}_6\text{H}_4)^+$ upon CID. Moreover, the generation of the $\text{Ho}(\text{C}_6\text{H}_4\text{S})(\text{C}_6\text{H}_4)^+ + \text{HCl}$ is, according to the calculation, endothermic by 190.1 kJ/mol (for more structural details of $\text{Ho}(\text{C}_6\text{H}_4\text{S})(\text{C}_6\text{H}_4)^+$, see ESI†). Finally, the possible charge transfer product, $\text{C}_6\text{H}_4\text{SC}_6\text{H}_4^+$, was not observed, in line with the much higher ionization energy of dibenzothiophene (8.44 eV^{29}) as compared to that of holmium (6.0 eV^{30}).

Two chemically plausible pathways, (a) and (b), are proposed for the generation of $\text{Ho}(\text{C}_6\text{H}_4\text{SC}_6\text{H}_4)^+$ possessing a $\text{C}_6\text{H}_4\text{SC}_6\text{H}_4$ ligand as illustrated in Scheme 1; both routes are initiated by σ bond metathesis under cleavage of the Ho-S and Ho-C bonds of the complex $\text{Ho}(\text{C}_6\text{H}_4\text{S})^+$, respectively. The PESs and the structural information of the associated intermediates and transition structures for the two pathways are shown in Fig. 3, and the encounter complex **9** serves as a common starting point. The TS for the Ho-S bond cleavage (**TS9/10**) is much higher in energy relative to the entrance channel as well as to the alternative Ho-C bond cleavage proceeding via **TS9/11** (61.7 kJ/mol versus -17.5 kJ/mol), i.e. dehydrochlorination is accessible under thermal conditions only via path (b) (**9** \rightarrow **TS9/11** \rightarrow **11**); therefore, it is only this route which has been considered further in the calculations of the subsequent reaction steps. The reason for the much higher barrier of the Ho-S bond cleavage (**TS9/10**) as compared to the Ho-C bond (**TS9/11**) is probably related to the stronger Ho-S bond compared to the Ho-C bond reflecting electronegativity differences between sulfur and carbon; unfortunately, the respective bond-dissociation energies are



Scheme 1 Plausible pathways for the generation of $\text{Ho}(\text{C}_6\text{H}_4\text{SC}_6\text{H}_4)^+$.

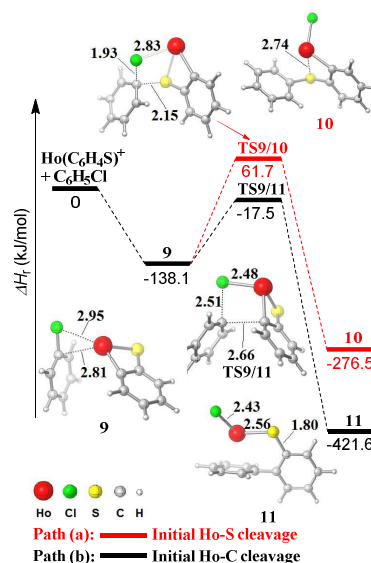


Fig. 3 PESs and structural information of the associated coordinates for the initial Ho-C and Ho-S cleavages of $\text{Ho}(\text{C}_6\text{H}_4\text{S})^+$ upon its reaction with chlorobenzene. Selected bond lengths are given in Å; charges are omitted for the sake of clarity.

not reported in the literature.

Subsequent to the formation of intermediate **11**, dehydrochlorination proceeds either directly via a hydrogen atom transfer from an *ortho*- position of the phenyl ring to the chloride ligand (**11** → **12**), or may be preceded by hydrogen scrambling within the original chlorobenzene entity (**11** → **13** → **14** → **15** → **16**). The PESs for these processes and structural information of the associated intermediates and transition structures for the generation of $\text{Ho}(\text{C}_6\text{H}_4\text{SC}_6\text{H}_4)^+$ as well as the intermediates for hydrogen scrambling along $\mathbf{13} \rightleftharpoons \mathbf{16}$ are shown in Fig. 4; structural details of the transition structures involved in the hydrogen scrambling are given in ESI†. According to the calculations, hydrogen scrambling is less energy demanding than the loss of HCl. The H/D scrambling has been verified by labeling experiments: in the reactions of $\text{Ho}(\text{C}_6\text{H}_4\text{S})^+$ with 3,5-*d*₂-1-chlorobenzene and 4-*d*-1-chlorobenzene, eliminations of both HCl and DCl are observed for either substrate; the ratios of HCl/DCl elimination from 3,5-*d*₂-1-chlorobenzene and from 4-*d*-1-chlorobenzene amount to 84:16 and 87:13, respectively. To quantitatively analyse these results in a kinetic modeling³¹⁻³⁵, hydrogen migration along the phenyl ring is treated as a complete H/D scrambling processes; further, the ratio for a *direct* HCl/DCl elimination *versus* H/D scrambling prior to HCl/DCl elimination as well as a kinetic isotope effect (*KIE*) have been fitted to the experimental data for both isotopologues. It turned out that the experimental data can be best modeled with assuming *KIE* = 1 and a

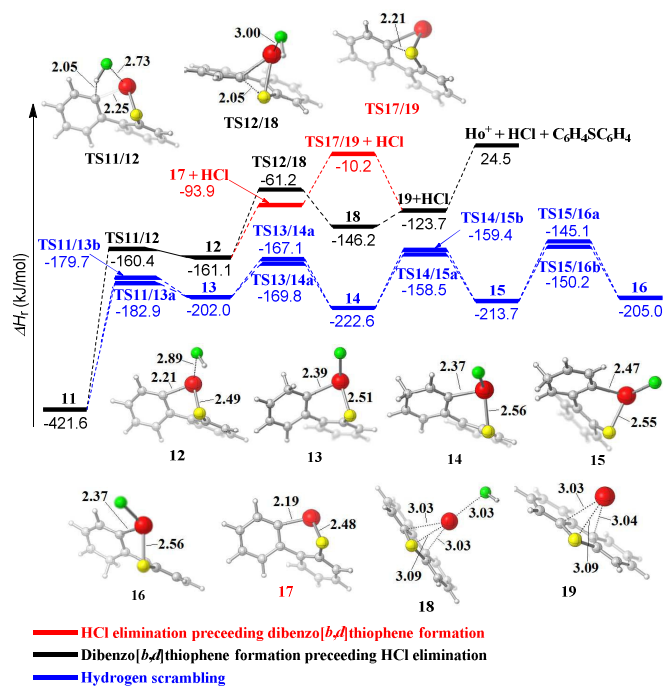
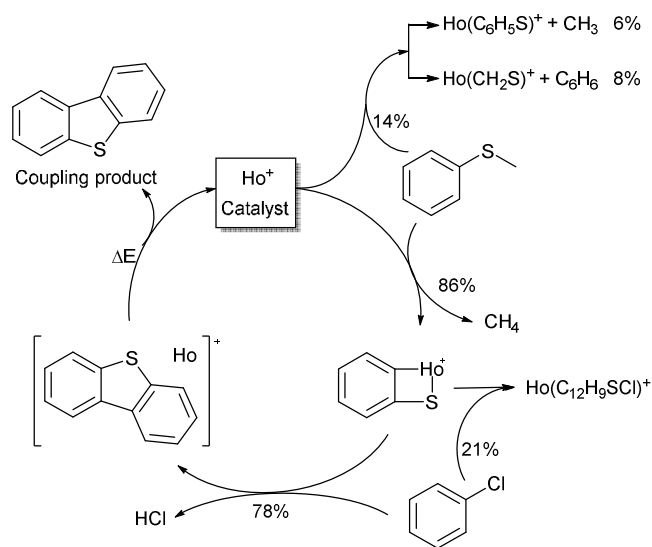


Fig. 4 PESs of the reactions starting from intermediate **11** as well as the structural information of some key coordinates; the notations **a** and **b** for the transition structures stand for the hydrogen migrations on both sites of the ring, respectively. Selected bond lengths are given in Å; charges are omitted for the sake of clarity. For further structural information, see Fig. 2 of ESI†.

branching ratio of 45% for H/D scrambling processes *versus* direct HCl/DCl elimination. A *KIE* = 1 is in agreement with the theoretical results, in that C–H(D) bond activation does not correspond to the rate-limiting step in the liberation of H(D)Cl and the generation of $\text{Ho}(\text{C}_6\text{H}_4\text{SC}_6\text{H}_4)^+$.

After having formed **12**, the next step corresponds to the construction of the thiophene ring; there are two variants in regard to the loss of HCl which can occur before or after the ring closure. The direct formation of the thiophene ring proceeds via **TS12/18** to form **18**, and subsequent elimination of HCl generates **19**; alternatively, direct liberation of HCl from **12** gives rise to **17** which subsequently rearranges via **TS17/19** to the complex **19** (see Fig. 4); both processes are accessible at thermal conditions. Thus, according to the calculation, the observed ionic product $\text{Ho}(\text{C}_6\text{H}_4\text{SC}_6\text{H}_4)^+$ may correspond to a mixture of **17** and **19**. Regarding the formation of $\text{Ho}^+ + \text{HCl} + \text{C}_6\text{H}_4\text{SC}_6\text{H}_4$, reaction (6), this has been calculated to be higher in energy by 25 kJ/mol as compared to the entrance channel, i.e. $\text{Ho}(\text{C}_6\text{H}_4\text{S})^+ + \text{C}_6\text{H}_5\text{Cl}$, and should thus not be observed under thermal conditions. Thus, assuming that the ions in the experiments are thermalized to room temperature possessing a kinetic energy of $3RT = 7.4$ kJ/mol at 298 K, theory overestimates the relative energy of the exit channel.

Considering the overall process, i.e. $\text{Ho}^+ + \text{C}_6\text{H}_5\text{SCH}_3 + \text{C}_6\text{H}_5\text{Cl} \rightarrow \text{Ho}^+ + \text{HCl} + \text{C}_6\text{H}_4\text{SC}_6\text{H}_4$, the atomic holmium cation Ho^+ serves as a catalyst, as illustrated in Scheme 2. However, the turnover number is limited by side reactions with both substrates (processes (2), (3), and (5)), and the turn-over frequency is diminished due to the inefficient release of the neutral coupling product from **19** under the regeneration of Ho^+ ions to initiate the next catalytic cycle. As so often in heterogeneous catalysis, product release and regeneration of the active catalyst (i.e. Ho^+) requires external energy³⁶⁻⁴¹. In addition, the presence of both substrates



Scheme 2 Catalytic cycle for the coupling of thioanisole and chlorobenzene mediated by atomic Ho^+ as well as side reactions.

thioanisole and chlorobenzene at the same time in a “one-pot synthesis” allows for additional side reactions as Ho^+ can react with both precursors. Moreover, $\text{Ho}(\text{C}_6\text{H}_4\text{S})^+$ can also react further with thioanisole to give higher order products. Thus, timing of the interaction of the catalyst with the two substrates needs to be well designed to improve the efficiency of the coupling process.

Conclusion

In this work, we present a novel gas-phase coupling of thioanisole and chlorobenzene to dibenzothiophene catalyzed by “bare” holmium cation Ho^+ and we address mechanistic aspects by DFT calculations and labeling experiments. The coupling is achieved via a two-step reaction: the first one corresponds to the reaction of Ho^+ with thioanisole to generate $\text{Ho}(\text{C}_6\text{H}_4\text{S})^+$; subsequently, $\text{Ho}(\text{C}_6\text{H}_4\text{S})^+$ reacts with chlorobenzene to produce the final products. A combination of experimental and computational investigations, provides insight into the most likely reaction mechanisms. For the overall transformation, atomic Ho^+ serves as a catalyst which, however, is also engaged in side reactions with both substrates. Similar to heterogeneous catalysis, external energy is required to release the coupling product from the catalyst.

Acknowledgement

Generous financial support by the *Fonds der Chemischen Industrie* and the *Deutsche Forschungsgemeinschaft* (“UniCat”) is appreciated. We thank Dr. Thomas Weiske for technical assistance.

Notes and references

- P. Y. Huang, L. H. Chen, Y. Y. Chen, W. J. Chang, J. J. Wang, K. H. Lii, J. Y. Yan, J. C. Ho, C. C. Lee, C. Kim and M. C. Chen, *Chem. Eur. J.*, 2013, **19**, 3721-3728.
- E. L. Ratcliff, R. C. Bakus, G. C. Welch, T. S. van der Poll, A. Garcia, S. R. Cowan, B. A. MacLeod, D. S. Ginley, G. C. Bazan and D. C. Olson, *J. Mater. Chem. C*, 2013, **1**, 6223-6234.
- C. Freund, W. Porzio, U. Giovanella, F. Vignali, M. Pasini, S. Destri, A. Mech, S. Di Pietro, L. Di Bari and P. Mineo, *Inorg. Chem.*, 2011, **50**, 5417-5429.
- C. Greco, G. Moro, L. Bertini, M. Biczysko, V. Barone and U. Cosentino, *J. Chem. Theory Comput.*, 2014, **10**, 767-777.
- C. D. Jones, M. G. Jevnikar, A. J. Pike, M. K. Peters, L. J. Black, A. R. Thompson, J. F. Falcone and J. A. Clemens, *J. Med. Chem.*, 1984, **27**, 1057-1066.
- J. K. Chakrabarti, T. M. Hotten, and D. E. Tupper, US5229382A, 1990.
- S. Martin-Santamaria, J. J. Rodriguez, S. de Pascual-Teresa, S. Gordon, M. Bengtsson, I. Garrido-Laguna, B. Rubio-Viqueira, P. P. Lopez-Casas, M. Hidalgo, B. de Pascual-Teresa and A. Ramos, *Org. Biomol. Chem.*, 2008, **6**, 3486-3496.
- E. Bey, S. Marchais-Oberwinkler, M. Negri, P. Kruchten, A. Oster, T. Klein, A. Spadaro, R. Werth, M. Frotscher, B. Birk and R. W. Hartmann, *J. Med. Chem.*, 2009, **52**, 6724-6743.
- A. R. Katritzky, R. A. Barcock, E. S. Ignatchenko, S. M. Allin, M. Siskin and C. W. Hudson, *Energ. Fuel.*, 1997, **11**, 150-159.
- C. L. Sun, Y. F. Gu, W. P. Huang and Z. J. Shi, *Chem. Commun.*, 2011, **47**, 9813-9815.
- R. Samanta and A. P. Antonchick, *Angew. Chem. Int. Ed.*, 2011, **50**, 5217-5220.
- R. Che, Z. Wu, Z. Li, H. Xiang and X. Zhou, *Chem. Eur. J.*, 2013, **20**, 7258-7261.
- Y. L. Mao and V. Boekelheide, *Proc. Natl. Acad. Sci. USA*, 1980, **77**, 1732-1735.
- M. Black, J. I. G. Cadogan and H. McNab, *J. Chem. Soc., Chem. Comm.*, 1990, 395-396.
- L. Benati, R. Leardini, M. Minozzi, D. Nanni, P. Spagnolo, S. Strazzari and G. Zanardi, *Org. Lett.*, 2002, **4**, 3079-3081.
- G. K. S. Prakash, C. Weber, S. Chacko and G. A. Olah, *Org. Lett.*, 2007, **9**, 1863-1866.
- M. Black, J. I. G. Cadogan and H. McNab, *Org. Biomol. Chem.*, 2010, **8**, 2961-2967.
- W. You, X. Y. Yan, Q. A. Liao and C. J. Xi, *Org. Lett.*, 2010, **12**, 3930-3933.
- T. H. Jepsen, M. Larsen, M. Jorgensen, K. A. Solanko, A. D. Bond, A. Kadziola and M. B. Nielsen, *Eur. J. Org. Chem.*, 2011, 53-57.
- Z. J. Qiao, H. Liu, X. Xiao, Y. N. Fu, J. P. Wei, Y. X. Li and X. F. Jiang, *Org. Lett.*, 2013, **15**, 2594-2597.
- M. M. Basher, Y. E. Corilo, R. Sparrapan, M. Benassi, R. Augusti, M. N. Eberlin and J. M. Riveros, *J. Mass Spectrom.*, 2012, **47**, 1526-1535.
- S. Zhou, M. Schlangen and H. Schwarz, *Chem. Eur. J.*, 2015, **21**, 2123-2131.
- D. K. Bohme and H. Schwarz, *Angew. Chem. Int. Ed.*, 2005, **44**, 2336-2354.
- H. Schwarz, *Isr. J. Chem.*, 2014, **54**, 1413-1431.
- X. F. Yang, A. Q. Wang, B. T. Qiao, J. Li, J. Y. Liu and T. Zhang, *Acc. Chem. Res.*, 2013, **46**, 1740-1748.
- M. T. Bowers and J. B. Ludenlager, *J. Chem. Phys.*, 1972, **56**, 4711-4712.
- V. Blagojevic, E. Flaim, M. J. Y. Jarvis, G. K. Koyanagi and D. K. Bohme, *Int. J. Mass Spectrom.*, 2006, **249**, 385-391.
- Y.-R. Luo, *Comprehensive Handbook of Chemical Bond Energies*, CRC Press, Boca Raton, 2007.
- J. K. Terlouw, W. Heerma, P. C. Frintrop, G. Dijkstra and H. A. Meinema, *J. Organomet. Chem.*, 1974, **64**, 205-221.
- R. J. Ackermann, E. G. Rauh and R. J. Thorn, *J. Chem. Phys.*, 1976, **65**, 1027-1031.
- D. Schroder and H. Schwarz, *Angew. Chem. Int. Ed.*, 1990, **29**, 1431-1433.
- D. Schroder, R. Brown, P. Schwerdtfeger and H. Schwarz, *Int. J. Mass Spectrom.*, 2000, **203**, 155-163.
- J. R. Brown, P. Schwerdtfeger, D. Schroder and H. Schwarz, *J. Am. Soc. Mass Spectrom.*, 2002, **13**, 485-492.
- J. Loos, D. Schroder and H. Schwarz, *J. Org. Chem.*, 2005, **70**, 1073-1076.
- B. Butschke, D. Schroder and H. Schwarz, *Organometallics*, 2009, **28**, 4340-4349.
- C. Bianchini, K. G. Caulton, C. Chardon, O. Eisenstein, K. Folting, T. J. Johnson, A. Meli, M. Peruzzini, D. J. Rauscher, W.

- E. Streib and F. Vizza, *J. Am. Chem. Soc.*, 1991, **113**, 5127-5129.
37. R. Wesendrup and H. Schwarz, *Organometallics*, 1997, **16**, 461-466.
38. B. Chiavarino, M. E. Crestoni and S. Fornarini, *Chem. Eur. J.*, 2002, **8**, 2740-2746.
39. T. Waters, R. A. J. O'Hair and A. G. Wedd, *J. Am. Chem. Soc.*, 2003, **125**, 3384-3396.
40. S. M. Lang, T. M. Bernhardt, R. N. Barnett and U. Landman, *Angew. Chem. Int. Ed.*, 2010, **49**, 980-983.
41. A. A. Lysova and I. V. Koptug, *Chem. Soc. Rev.*, 2010, **39**, 4585-4601.